Received: 29 October 2020 | Revised: 22 January 2021 | Accepted: 3 February 2021

DOI: 10.1111/gcb.15557

Global Change Biology WILEY

PRIMARY RESEARCH ARTICLE

Drought alters the carbon footprint of trees in soils—tracking the spatio-temporal fate of ^{13}C-labelled assimilates in the soil of an old-growth pine forest

Decai Gao[1,2] | Jobin Joseph[1] | Roland A Werner[3] | Ivano Brunner[1] | Alois Zürcher[1] | Christian Hug[1] | Ao Wang[1,4] | Chunhong Zhao[2] | Edith Bai[2] | Katrin Meusburger[1] | Arthur Gessler[1,4] | Frank Hagedorn[1]

[1]Swiss Federal Research Institute WSL, Birmensdorf, Switzerland

[2]Key Laboratory of Geographical Processes and Ecological Security of Changbai Mountains, Ministry of Education, Northeast Normal University, Changchun, China

[3]Department of Environmental Systems Science, ETH Zurich, Zurich, Switzerland

[4]Terrestrial Ecosystems, ETH Zurich, Zurich, Switzerland

Correspondence
Frank Hagedorn, Swiss Federal Research Institute WSL, Birmensdorf, Switzerland.
Email: frank.hagedorn@wsl.ch

Funding information
Swiss National Science Foundation, Grant/Award Number: 31003A_159866 and 310030_189109; Sino Swiss Science and Technology Cooperation, Grant/Award Number: EG 09-122016

Abstract

Above and belowground compartments in ecosystems are closely coupled on daily to annual timescales. In mature forests, this interlinkage and how it is impacted by drought is still poorly understood. Here, we pulse-labelled 100-year-old trees with $^{13}CO_2$ within a 15-year-long irrigation experiment in a naturally dry pine forest to quantify how drought regime affects the transfer and use of assimilates from trees to the rhizosphere and associated microbial communities. It took 4 days until new ^{13}C-labelled assimilates were allocated to the rhizosphere. One year later, the ^{13}C signal of the 3-h long pulse labelling was still detectable in stem and soil respiration, which provides evidence that parts of the assimilates are stored in trees before they are used for metabolic processes in the rhizosphere. Irrigation removing the natural water stress reduced the mean C residence time from canopy uptake until soil respiration from 89 to 40 days. Moreover, irrigation increased the amount of assimilates transferred to and respired in the soil within the first 10 days by 370%. A small precipitation event rewetting surface soils altered this pattern rapidly and reduced the effect size to +35%. Microbial biomass incorporated 46 ± 5% and 31 ± 7% of the C used in the rhizosphere in the dry control and irrigation treatment respectively. Mapping the spatial distribution of soil-respired $^{13}CO_2$ around the 10 pulse-labelled trees showed that tree rhizospheres extended laterally 2.8 times beyond tree canopies, implying that there is a strong overlap of the rhizosphere among adjacent trees. Irrigation increased the rhizosphere area by 60%, which gives evidence of a long-term acclimation of trees and their rhizosphere to the drought regime. The moisture-sensitive transfer and use of C in the rhizosphere has consequences for C allocation within trees, soil microbial communities and soil carbon storage.

KEYWORDS
carbon allocation, climate change, drought, forest, isotope tracing, mean, residence time, rhizosphere, roots, soil respiration

1 | INTRODUCTION

Water is essential for all organisms and thus, the increasing intensity and frequency of drought in large areas of the Northern hemisphere is impacting the diversity and functioning of forest ecosystems. In Central Europe, for instance, net ecosystem C uptake decreased in the extremely hot and dry year 2003 (Ciais et al., 2005) and forest health suffered and productivity declined in response to the dry summer 2018 (Buras et al., 2020). Climate projections indicate an exacerbation of the drought regime, with average summer precipitation expected to decrease by 25% in Central Europe until the end of 21st century (Stocker et al., 2014).

Impacts of drought on ecosystems range from immediate reductions of the metabolic activity of plants and soil organisms and the acclimation of physiological processes to species shifts under prolonged or reoccurring drought (Frank et al., 2015; Hagedorn et al., 2016; Reichstein et al., 2013; Schimel, 2018). The interrelation of different ecosystem processes and in particular the coupling of the above- and belowground system is one of the critical unknowns in predicting drought effect on ecosystems (Frank et al., 2015; von Rein et al., 2016). Especially limited knowledge exists in mature forests where these processes are difficult to quantify, and timescales of C metabolization within trees and the C transfer among tree compartments can range between days and decades (Herrera-Ramírez et al., 2020). Up to 50% of recent tree photosynthates are assumed to be transferred within a few days from trees into the belowground compartment (Epron et al., 2011; Högberg et al., 2008; Joseph et al., 2020), where they fuel root processes and soil microbial communities living in close association with the roots (Epron et al., 2012; Hagedorn et al., 2016). In mature trees, phloem transport leads to distinct time lags in plant–soil coupling (Dannoura et al., 2011; Kuzyakov & Gavrichkova, 2010) and a substantial fraction of assimilates is intermediately stored in the wood parenchyma before it is used for respiratory processes (Muhr et al., 2013). So far, it remains uncertain to which extent this 'pre-aged' C is transferred and used in the rhizosphere as pulse-labelling experiments have been mostly confined to only a few weeks (e.g. Epron et al., 2011). However, relative old radiocarbon ages of newly formed fine roots (Solly et al., 2018) indicate that a substantial fraction of C used in the rhizosphere consists of C that has been assimilated several years earlier.

Drought affects the use and partitioning of C in the plant and soil systems at different timescales by immediately influencing the sink and source activity of plants and associated belowground communities, by altering the formation of osmolytic and storage compounds and by long-term adjustments of the root-to-shoot ratios (Brunner et al., 2015; Gessler et al., 2017; Manzoni et al., 2012). For saplings and young trees, experimental drought was found to decrease C allocation of recently assimilated C to their rhizosphere and associated microorganisms, either through a decreasing C demand of the rhizobiome or through a reduced photosynthetic CO_2 uptake (Barthel et al., 2011; Hagedorn et al., 2016; Ruehr et al., 2009). Upon rewetting, however, this decline in allocation during drought was compensated by an enhanced transfer of assimilates to the belowground, partly to regain rhizosphere functioning (Hagedorn et al., 2016; Ruehr et al., 2019). At the annual to decadal timescale, plants are adjusting their rooting system to the water limitation and the altered water demand of the aboveground compartment. In general, plants give priority to roots when water (or nutrients) are limiting which leads to consistent increases of the root-to-shoot ratio under drought (Poorter et al., 2012). However, fine root biomass shows variable responses that seem to depend on the severity of drought (Brunner et al., 2015). While mild drought frequently increases C allocation belowground (Gaul et al., 2008), more severe and long-lasting drought was observed to lead to a decrease (Hommel et al., 2016). These acclimative allocation and growth adjustments under drought will also impact the C transfer from plants to soils, but these indirect legacy effects remain unknown for forests. For grasslands, Fuchslueger et al. (2016) showed that drought history and hence the acclimation of grasslands to previous drought events decreased the allocation of assimilates to the rhizosphere and associated microbial communities—the detailed mechanism remained elusive.

Our study aimed at assessing the impact of reoccurring natural drought on the transfer of recent assimilates from canopies of mature trees to their rhizosphere at various timescales. We applied $^{13}CO_2$ pulses to entire canopies of ten 100-year-old pine trees and tracked the ^{13}C signal in soil-respired CO_2 and microbial biomass for 1 year. The pulse-labelling experiment was conducted in a naturally dry pine forest where in parts of the stand the water limitation had been removed by a 13-year-long experimental irrigation (Schönbeck et al., 2018). Pulse labelling of both, irrigated (n = 5) and control (n = 5) trees, was performed in time blocks before and after intermittent rainfall events, which allowed us to assess the impacts of various drought regimes—ranging from water shortage in the naturally dry control, its short-term modulation by intermittent precipitation events and its removal by long-term irrigation. We measured the soil respiratory ^{13}C signal at various distances from the trees enabling us to map the spatial extent of the respiratory active rhizosphere and thus to estimate the long-term acclimation of the rhizosphere to reoccurring summer drought. Our hypotheses were that in this naturally dry pine forest (1) the velocity and magnitude of the allocation of recent assimilates to the belowground decreases with decreasing soil moisture, primarily due to a declining C demand of the rhizobiome and that (2) the difference between the irrigated and the natural dry site is reinforced by the 15-year-long tree growth stimulation through irrigation leading to a greater rhizosphere.

2 | MATERIALS AND METHODS

2.1 | Site description and long-term irrigation experiment

The ^{13}C pulse-labelling experiment was conducted within a long-term irrigation experiment that started in summer 2003 and is located in the Rhone Valley near Leuk, Canton Valais, Switzerland (46°18′N, 7°37′E, 615 m a.s.l.). The forest is dominated by adult,

approximately 100-year-old Scots pine (*Pinus sylvestris*) with interspersed pubescent oak (*Quercus pubescens*) and has a stem density of 730 trees per hectare (Rigling et al., 2013). The study area is characterized by a moderately continental climate with a mean annual temperature of 10.7°C and a mean annual precipitation of 518 mm (Herzog et al., 2014) and is located at the dry edge of distribution of Scots pine. In the past 30 years, Scots pine mortality events occurred regularly in this area (Bigler et al., 2006) The soil type is a shallow approx. 20 cm thick Pararendzina developed on an alluvial fan (Hartmann et al., 2017).

For the long-term irrigation experiment, the experimental site (~1 ha) was split up into eight plots of 1000 m^2 each that are separated by a 5-m buffer area (Herzog et al., 2014). Four randomly selected plots (further termed 'irrigated') were irrigated by sprinklers with 5 mm per day during the vegetation period (from May to October), which approximately doubles the rainfall compared to the other four plots under naturally dry conditions (further termed 'dry control'). The irrigation water was taken from an adjacent channel of the river Rhone that is hydrologically disconnected from the surrounding soil (Schönbeck et al., 2018).

2.2 | ^{13}C pulse labelling

In late summer 2017, we conducted a whole crown ^{13}C pulse-labelling experiment with 10 trees, five of the dry control plots and five of the irrigated plots. Access to the 10- to 12-m high tree canopies was provided by large scaffolds that have been built in the forest. For the pulse labelling, the whole tree canopy of each tree was wrapped in a large transparent plastic bag and highly ^{13}C-enriched CO_2 (^{13}C excess atom fraction 0.99); ^{13}C (Cambridge Isotopes) was released to each tree for 3.5 h (Figure 1). The concentration of $^{13}CO_2$ and $^{12}CO_2$ in the sealed plastic bag was monitored with an isotope laser spectrometer (LGR, CCIA 46d, LosGatos Research Ltd) and kept manually at about 1500 ppm (with a carbon isotopic composition of the CO_2 of approx. 75 atom-%), which exceeded the saturation point of plant CO_2 uptake (Joseph et al., 2020). Temperature in the plastic bag during labelling was adjusted to ambient temperature by an air conditioner placed on the scaffolds. After labelling, the plastic bags were removed and strong industrial blowers were used to flush the labelled $^{13}CO_2$ gas away and to prevent the labelled ^{13}C-CO_2 gas to sink to the ground and diffuse into the soils as well to be taken up by the understorey vegetation. The pulse labelling was conducted pairwise and every day one tree from a dry control and one from an irrigated plots were labelled with ^{13}C-enriched CO_2. The labelling was started in the end of August 2017 when the control plots experienced a moderate drought. A small precipitation event interrupted the pulse labelling and retarded the labelling of the remaining two pairs by 8 days. Overall, this resulted in two time blocks with three tree pairs before the precipitation event (n = 6 trees) and two pairs after it (n = 4 trees). Canopy sizes and tree heights of pulse-labelled trees were measured with a laser-based ruler.

2.3 | CO_2 flux rates from soil and stem, and soil sampling

Soil CO_2 fluxes and their carbon isotopic signatures were measured from polyvinyl chloride (PVC) collars (10.5 cm in diameter) inserted into the soil to 3 cm depth along three transects from each of the labelled tree at distances of 0.5, 1, 2, 3, 4, 6 and 8 m from the tree trunk (n = 21 per tree). Rates of soil CO_2 flux were measured with a Li-8100A soil CO_2 flux system with a LI 8100-102 survey chamber (LI-COR INC.). In parallel, soil temperature at 5 cm was measured with a portable thermometer. At the same day, the $\delta^{13}C$ values of soil-respired CO_2 were analysed using the closed-chamber method,

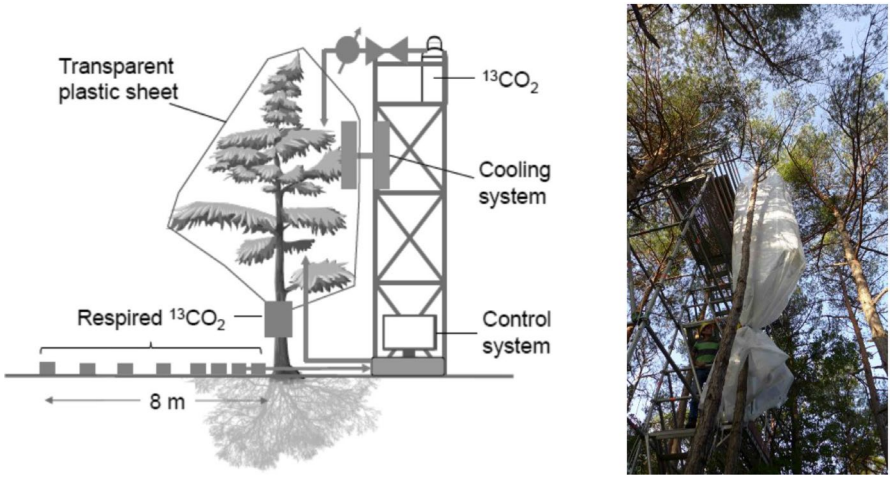

FIGURE 1 Experimental set-up of the $^{13}CO_2$ pulse labelling of mature pine trees and the spatio-temporal ^{13}C tracking in stem and soil-respired CO_2 using soil collars placed at several distances in three directions from each tree stem. The $^{13}CO_2$ addition was adjusted with a mass flow controller based on continuous $^{13}CO_2$ measurements using a laser spectrometer. Overall 10 approximately 100-year-old pine trees were pulse-labelled, five of them growing under naturally dry conditions and five under irrigation. Adapted from Joseph et al. (2020)

where each chamber was closed for 15–30 min with a PVC-Lid (depending on the efflux rates). Gas samples were taken with a syringe at the beginning and end of the closure and transferred in 12-ml glass vials ('exetainer', Labco) for measuring their $\delta^{13}C$ values. Two additional samples were taken from ambient air near the soil collars of each tree. Gas samples were taken before labelling and 2, 3, 4, 6, 10, 15, 20 and 30 days as well as 8, 10, 11, 12 and 13 months after labelling. Gas samples were analysed with a modified gas bench II (Zeeman et al., 2008) that was combined with a Delta^{plus}XP mass spectrometer (Thermo Fisher).

$\delta^{13}C_{resp}$ was calculated with the following equation (Hagedorn et al., 2012).

$$\delta^{13}C_{resp} = \left(\delta^{13}C_{chamber} \times C_{chamber} - \delta^{13}C_{ambient} \times C_{ambient}\right) / \left(C_{chamber} - C_{ambient}\right), \quad (1)$$

where $\delta^{13}C_{chamber}$ and $\delta^{13}C_{ambient}$ are the $\delta^{13}C$ values in the soil chamber and the ambient air, and $C_{chamber}$ and $C_{ambient}$ are the CO_2 concentrations in the chamber and the ambient air respectively. In addition, $\Delta\delta^{13}CO_2$ was calculated using the difference of the $\delta^{13}CO_2$ value between soil collars influenced by the pulse labelling and ambient ones outside the labelling area.

In 2018, the $\delta^{13}CO_2$ values of stem-respired CO_2 were also measured by wrapping the stems in a height of ca. 1.5 m with plastic foliar, sealing it with tape and taking gas samples 1 day after closure. The $\delta^{13}C_{resp}$ and $\Delta\delta^{13}CO_2$ of stem-respired CO_2 were calculated as the difference in $\delta^{13}C$ values of CO_2 between ^{13}C-labelled and unlabelled trees.

Soils were sampled on the same day when CO_2 efflux rates were measured. The soil samples were collected at three depth layers after removing the litter layer: 0–2, 2–5 and 5–10 cm. For each tree, samples were taken at 12 points within 1-m distance from the trunk of each labelled tree evenly distributed among the directions of the three transects for CO_2 flux measurements using a 2-cm diameter soil auger. All samples per tree and depth were bulked homogeneously. Over the entire sampling campaign encompassing 10 sampling dates, a total of 120 soil samples was collected for each tree. Soils were immediately processed by removing roots using a 4-mm sieve and freezing sieved soils. Soil gravimetric water content was measured by drying soil aliquots at 105°C for 24 h.

2.4 | Soil microbial biomass carbon

Soil microbial biomass carbon (MBC) and soil extractable organic C (EOC) were determined using a chloroform fumigation-extraction method after unfreezing the soils (Vance et al., 1987). The fumigated and unfumigated soil samples were extracted with a 0.5 M K_2SO_4 solution (fresh soil: 0.5 M K_2SO_4 solution = 1:4, end-over-end shaking 1 h). The obtained soil solutions were used to analyse the $\delta^{13}C$ values and corresponding carbon concentrations according to Lang et al. (2012). Briefly, 1 ml of the soil extract and 1 ml of oxidizing agent (4.0 g $K_2S_2O_8$ + 200 µl of 85% H_3PO_4 + 100 ml of distilled water) were added in 12-ml vials. After that, the CO_2 present in the vial headspace and acidified samples was removed with high-purity helium (Grade 5.0 99.999% He). To accomplish oxidation, the sample vials were placed in aluminium blocks to oxidize dissolved organic C to CO_2 (at 100°C for 60 min). Finally, the $\delta^{13}C$ values and the C concentrations of the evolved CO_2 samples were measured using a modified GasBench II coupled to an Isotope Ratio Mass Spectrometer.

The concentration of MBC was calculated as the difference of organic C between fumigated and unfumigated soil divided by a factor of 0.45 (Vance et al., 1987). The pool of microbial biomass on an area basis was estimated by multiplying microbial biomass with the mass of soil on an area base using measured soil bulk densities. The $\delta^{13}C$ of MBC was calculated with the following mass balance equation:

$$\delta^{13}C_{MBC} = \left(\delta^{13}C_f \times C_f - \delta^{13}C_{nf} \times C_{nf}\right) / \left(C_f - C_{nf}\right), \quad (2)$$

where $\delta^{13}C_f$ and $\delta^{13}C_{nf}$ are the values of $\delta^{13}C$-EOC in the fumigated and unfumigated soils, and C_f and C_{nf} are the concentrations of EOC in the fumigated and unfumigated soils respectively.

2.5 | Calculation of soil CO_2 effluxes and ^{13}C mass balance

Total soil CO_2 effluxes during the first 30 days following the pulse labelling were estimated by interpolating linearly between daily measurements. After that, we interpolated soil CO_2 effluxes between measurements by the temperature dependency of soil CO_2 effluxes from the irrigated plots assessed from 2011 to 2019 showing a Q_{10} value of 3.88 (Data S1). Soil CO_2 effluxes from irrigated soils were then calculated for each day using daily averages of continuously monitored soil temperatures at 10 cm. For soils of dry controls, we additionally considered the moisture limitation of soil CO_2 effluxes by first calculating the ratio between the fluxes from dry control and irrigated (non-water limited) plots and applying it to continuously monitored volumetric soil water contents for the dry summer months 2018.

For assessing the ^{13}C mass balance, we first estimated the amount of ^{13}C by converting the $\delta^{13}C$ value (relative to the Vienna PeeDee Belemnite, VPDB) to atom fraction in % (also named atom %)

$$\chi\left(^{13}C_P\right) = \frac{1}{1 + \left(1/\left(\delta^{13}C_{P/VPDB} + 1\right) \cdot 0.01117960\right)} \times 100, \quad (3)$$

where 0.01117960 is the international accepted $^{13}C/^{12}C$ ratio of the standard VPDB.

The total ^{13}C enrichment (*^{13}C excess atom fraction*, here abbreviated as *^{13}C excess*) for EOC, MBC or respired CO_2 was then determined as follows:

$$^{13}C\text{excess} = \left(\chi\left(^{13}C\right)_{P,\,sample} - \chi\left(^{13}C\right)_{P,\,blank}\right) / 100 \times F, \quad (4)$$

where $\chi(^{13}C)_{P,\,sample}$ and $\chi(^{13}C)_{P,\,blank}$ are the *atom fraction* (in %) of the samples determined at a given time point after $^{13}CO_2$ pulse labelling

and the natural abundance of ^{13}C respectively. F are the pools of EOC, MBC or the flux of respired CO_2.

The soil $^{13}CO_2$ flux from the entire rhizosphere of each pulse-labelled tree was estimated by interpolating ^{13}C excess of soil-respired CO_2 linearly between adjacent soil collars placed at various distances (e.g. between 1 and 2 m) from each of the tree stems. The flux during a given period was obtained by integrating these fluxes in time.

The visualization of $\delta^{13}C$ values in soil-respired CO_2 was conducted in two steps. At first, we estimated $\delta^{13}C$ values for 12 directions around each tree by interpolating values of the measured three transects for each distance class. Subsequently, the inverse distance weighting (IDW) interpolation technique and designed tool in ESRI ArcGIS 10.5 was used for visualization, considering $^{13}CO_2$ is a locational dependent variable. IDW interpolation determines values in places without on-ground measurement using a linearly distance-weighted combination of a set of observation points. The number of nearest input sample points to be used to perform interpolation was specified as 12. The measured point shape files were interpolated in raster format for 10 trees and 30 days following pulse labelling. Figure 7 shows the combined output.

The ^{13}C pool in microbial biomass in the rhizosphere of each pulse-labelled tree stem was obtained by first linking ^{13}C excess in microbial biomass measured at a distance of 1 m from each tree stem to the soil $^{13}CO_2$ flux at day 10 ($r^2 = 0.83$, $p < 0.001$; Figure S2) and then using the decline of the measured soil $^{13}CO_2$ flux with increasing distance from each stem to estimate ^{13}C excess at each location. In addition, we integrated these values over the entire area to yield the ^{13}C excess in microbial biomass for the rhizosphere of each pulse-labelled tree.

The *^{13}C uptake by trees* was estimated based on the amount of 99%^{13}C-CO_2 supplied to the pulse labelling chamber from the gas cylinder (Table 1). The fraction of ^{13}C taken up by trees being respired from the soil was calculated by dividing ^{13}C excess of soil-respired CO_2 by this value. The total recovery of ^{13}C in various compartments of tree biomass, CO_2 fluxes from tree canopy, stems and soil was 75% of the amount of ^{13}C assimilated (Joseph et al., 2020).

2.6 | Data and statistical analysis

The *time lag* between the pulse labelling and thus ^{13}C assimilation in the tree crown and the time of the first appearance of the ^{13}C signal in soil-respired CO_2 and microbial biomass as well the *peak time*, when ^{13}C signal of both parameters was maximal, were identified with the help of the Peak analyzer (OriginPro 2020). The lateral extension of ^{13}C respiration depicting rhizosphere respiration was estimated by first fitting ^{13}C excess of soil-respired CO_2 to the distance from tree stems using exponential functions. At the temporal ^{13}C peak (10 days after pulse labelling), we determined the *maximal extension of rhizosphere* along each transect from the tree trunks, by estimating when the $\Delta\delta^{13}C$-CO_2, the difference in $\delta^{13}C$ in soil-respired CO_2 between labelled and unlabelled soil, was 5‰. This value was regarded to reflect a significant ^{13}C signal originating from new assimilates and it equalled approximately 5% of the $\Delta\delta^{13}C$-CO_2 within the first meter from the trunks. The *highly active rhizosphere* of each tree was defined to be delimited by a $\Delta\delta^{13}C$-CO_2 of 25% of its maxima within the first m from the tree trunks. These radii were then used to calculate the rhizosphere area.

The temporal dynamics of ^{13}C signal in soil-respired CO_2 was estimated by fitting $\Delta\delta^{13}C$-CO_2 values after the ^{13}C peak to a one or two-pool model (Epron et al., 2012), with the latter being:

$$y = a_1 * \exp\left(-x/\tau_1\right) + a_2 * \exp\left(-x/\tau_2\right), \quad (5)$$

where a_1 and a_2 are the sizes of $\Delta\delta^{13}C$-CO_2 of the rapid cycling pool 1 [in ‰] and slow cycling pool 2 at time $t = 0$ ($\Delta\delta^{13}C$-CO_2 peak), τ_1 and τ_2 are the mean residence time (MRT=1/k, k = rate constant of decline in $\Delta\delta^{13}C$-CO_2) of the two pools [in days] and x is the time after the peak. X^2/DoF was chosen as a criterion to optimize the goodness of the fit as compared to the number of fitting parameters in the one- or two-pool model. The overall mean residence time $\tau_{Overall}$ of $\Delta\delta^{13}C$ in soil respiration of the two-pool model was then calculated based on the relative contribution of the two pools a_1 and a_2 (Equation 5) normalized to 1 (f_1 and f_2) and their mean residence times.

$$\tau_{overall} = f_1 * \tau_1 + f_2 * \tau_2. \quad (6)$$

The effect size of the irrigation treatment was calculated as percentage effect = (irrigated − control dry)/irrigated × 100. Linear mixed effects models employing maximum likelihood (lme function from the nlme package in R 3.5.3) were used to test the influence of the long-term water regime (irrigated vs. dry control, named *irrigation*) and the *timing* (first vs. second time block of labelling) separated by the intermittent precipitation event as fixed effects. p values were calculated according to Satterthwaite's approximations. Labelling pairs and individual tree were included as random effects. Models were run for all dates where the autocorrelation structure (corAR1 function in the nlme package) was included in the models to account for repeated measurements with a first-order autoregressive covariate structure. In addition, we tested cumulative values, specific periods and spatial patterns without the corAR1 function. For spatial pattern, we also included crown area as a co-variable. The dependent variables were log-transformed to improve normality and homoscedasticity of the residuals. All statistical analyses were performed using the R platform (version 3.5.3).

3 | RESULTS

3.1 | Soil moisture and soil respiration

In summer 2017, when the pulse labelling was carried out, precipitation from June to August was 190 mm, while it amounted only to 67 mm in summer 2018. As a result soil moisture contents

were higher in summer 2017 than in the hot and dry summer 2018. The daily irrigation during the vegetation period increased soil moisture significantly (Figure 2). During the pulse labelling in late summer 2017, an intermittent precipitation event in between the two blocks of pulse labelling and after the second one increased soil moisture in surface soils in both treatments (0–5 cm depth; $P_{Timing} < 0.05$).

Soil respiration showed a typical seasonal pattern with the highest rate in summer and strong increase by irrigation during the dry summer months ($P_{Irrigation} < 0.001$). During the pulse-labelling experiment in fall 2017, modelled soil CO_2 effluxes based on the long-term temperature and moisture dependency (Data S1) applied to continuously monitored soil temperatures and moisture were smaller than the measured ones in the dry control (Figure 2). The annual soil CO_2 efflux estimated by taking daily measurement for the first 30 days following pulse labelling and interpolating between measurements using temperature and moisture dependencies for the following 11 months yielded a flux of approximately 690 ± 47 and 1310 ± 98 g CO_2-C m^{-2} $year^{-1}$ from the dry control and the irrigated soils respectively.

3.2 | Temporal dynamics of newly assimilated C in soil-respired $^{13}CO_2$

The ^{13}C pulse added to the tree crowns started to appear in soil-respired CO_2 4 days after labelling, reaching a maximum value between the 6th and 10th day after labelling. Thereafter, the ^{13}C signal in soil-respired CO_2, depicted as $\Delta\delta^{13}C$-CO_2 and ^{13}C excess decreased exponentially to 20% of the ^{13}C peak 30 days after labelling (Figure 3; Table 1). The ^{13}C signal was still detectable 1 year later, shifting $\delta^{13}C$ values by 5 ± 1‰ as compared to ambient values (10 month data; Figure 4). Irrigation influenced the temporal dynamics of the ^{13}C signal in soil-respired CO_2, but the pattern depended on the timing of the pulse labelling (Figure 3). In the first time block of pulse labelling before the precipitation event, the ^{13}C signal under the irrigated trees was stronger and arrived 2.3 days earlier and also peaked earlier (6.8 ± 0.8 vs 8.5 ± 0.5 days) than in the dry controls (Table 1). In contrast, in the time block after the precipitation event, the ^{13}C signal in soil-respired CO_2 arrived 1.7 days earlier and peaked 2.5 days earlier in the dry control ($P_{Timing \times Irrigation} < 0.02$; Table 1). The time lag in ^{13}C appearing in soil-respired CO_2 when related to tree height provides an estimate of the velocity of the stem transport of recent assimilates (Table 1). Results showed that the average velocity was 2.6 m per day with irrigation accelerating stem transport ($P_{Irrigation} < 0.001$). Again, the irrigation effect became smaller after the intermittent precipitation event ($P_{Timing \times Irrigation} < 0.01$; Figure 5). Also, the response of the intensity of the ^{13}C signal in the soil, the $\Delta\delta^{13}C$-CO_2 ($\delta^{13}C_{labelled\ tree} - \delta^{13}C_{unlabelled\ tree}$) was opposite between the two time blocks of pulse labelling. Before the intermittent precipitation event, the peak of the $\Delta\delta^{13}C$-CO_2 in the first 3 m from the stems was 80% higher in the irrigated soils than in the unirrigated

TABLE 1 Spatio-temporal distribution of ^{13}C-labelled assimilates in soil-respired CO_2 and microbial biomass following pulse labelling of mature pine trees. Values were reported as means ± standard errors. Statistical significances were tested with linear mixed effects models

Timing	Treatment	^{13}C assimilation by trees (mg ^{13}C/tree)	^{13}C time lag of soil-respired CO_2 (days)	^{13}C peak time (days)	Mean residence time (days)	Transport velocity crown to rhizosphere (m/day)	^{13}C excess soil-respired CO_2 (first 10 days) (mg ^{13}C/tree/10 days)	Relative ^{13}C losses by soil respiration (during 1 year) (% of ^{13}C assimilated)	^{13}C excess in microbial biomass (at day 10) (mg ^{13}C/tree)	Contribution of microbial biomass to belowground ^{13}C allocation (%)	^{13}C excess in roots (after 30 days)[a] (mg ^{13}C/tree)
Before precipitation	Irrigated	9913 ± 946	4.0 ± 0.0	6.8 ± 0.8	39.6 ± 0.46	3.11 ± 0.11	678 ± 151	34.8 ± 4.6	315 ± 124	32.4 ± 13.2	696 ± 171
	Dry control	8200 ± 977	6.3 ± 0.3	8.5 ± 0.5	88.9 ± 13	1.84 ± 0.12	143 ± 12	24.6 ± 5.9	135 ± 55	44.7 ± 9	366 ± 159
After precipitation	Irrigated	13350 ± 58	4.5 ± 0.5	8.3 ± 0.3	36.3 ± 4.66	3.14 ± 0.07	709 ± 65	26.5 ± 1.4	289 ± 7	28.1 ± 4	1762 ± 780
	Dry control	11777 ± 776	4.0 ± 0.0	5.8 ± 0.3	48.9 ± 5.34	2.7 ± 0.2	526 ± 48	32.5 ± 1.0	509 ± 79	49 ± 6	2390 ± 462
Statistical significance	Timing	**0.043**	**0.018**	0.44	0.068	0.079	**0.026**	0.81	0.22	0.96	**0.026**
	Irrigation	0.187	**0.005**	0.91	**0.015**	**0.0008**	**0.009**	0.49	0.084	**0.019**	0.45
	Timing ×Irr.	0.76	**0.002**	**0.02**	0.14	**0.0062**	**0.047**	0.19	**0.01**	0.35	0.20

Bold indicates significant values ($p < 0.05$).

[a] Data from Joseph et al. (2020).

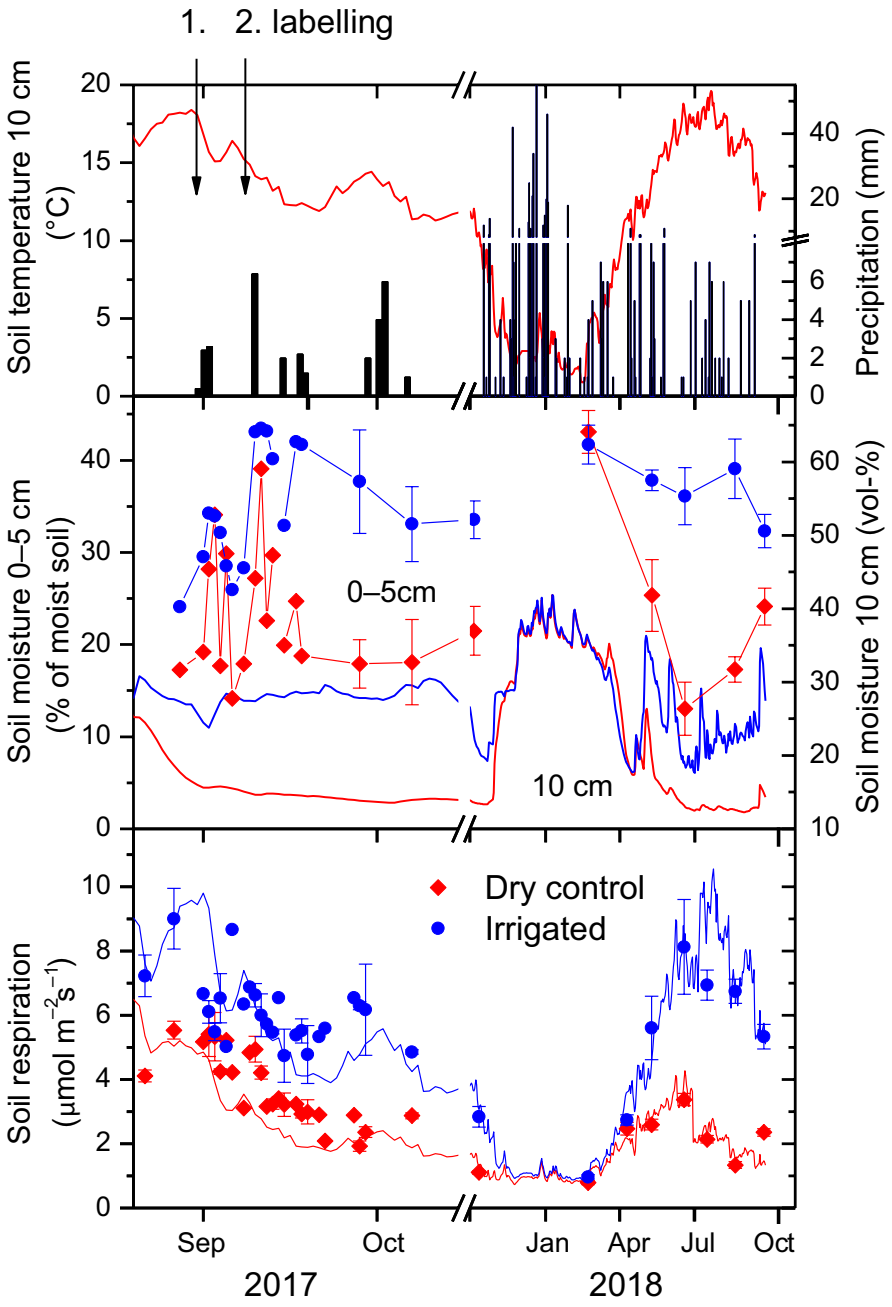

FIGURE 2 Temporal variations of soil temperature at 5 cm depth, precipitation (top panel), soil gravimetric water content at 0–5 cm (symbols) and soil volumetric water content at 10 cm depth (mid panel), and soil respiration (lower panel) under the irrigated (blue line) and the dry control (red line) treatments. For soil respiration, symbols represent measured fluxes, while lines show modelled ones. The vertical bars represent standard errors (SE). Arrows represent the dates of ^{13}C-CO_2 labelling. Note that x-axis has a higher temporal resolution for the first 2 months of the experiment

ones, but 45% smaller after it (Figure 3). Most interestingly, in 2018, in the year following the ^{13}C pulse labelling, the $\Delta\delta^{13}C$ in soil-respired CO_2 was about three times greater under the dry control trees than under irrigated trees ($P_{Irrigation} < 0.05$; Figure 4). The same pattern was found for stem respiration. However, as total soil CO_2 effluxes were greater under irrigation, the total efflux from the ^{13}C label (=^{13}C excess) did not differ between the treatments.

The overall temporal dynamics of the ^{13}C pulse in soil-respired CO_2 was best described by a two-pool model (Table S1). The overall MRT was faster under irrigation ($P_{Irrigation} < 0.02$) and showed a significant negative relationship with soil moisture at 0–5 cm depth in the first 4 days following pulse labelling (Figure 6).

3.3 | Spatial patterns of ^{13}C-based rhizosphere respiration

The spatial mapping of soil-respired ^{13}C reflecting rhizosphere respiration showed the highest rates in an area of approximately 1-m distance to the tree stems (Figure 7), from where the ^{13}C signal decreased exponentially to an average distance of 3.8 m, at which the ^{13}C signal was still detectable (Table 2). A few hot spots also existed at a distance of 6 m (Figure 7). The lateral extension of the highly *active* rhizosphere which we defined to have a $\Delta\delta^{13}C$-CO_2 above 25% of the ^{13}C peak height was 2.5 m. In comparison, tree canopies had an average radius of 1.29 ± 0.17 and 1.52 ± 0.21 in the dry control and irrigated treatment respectively. The size of the rhizosphere and tree crowns were significantly correlated with

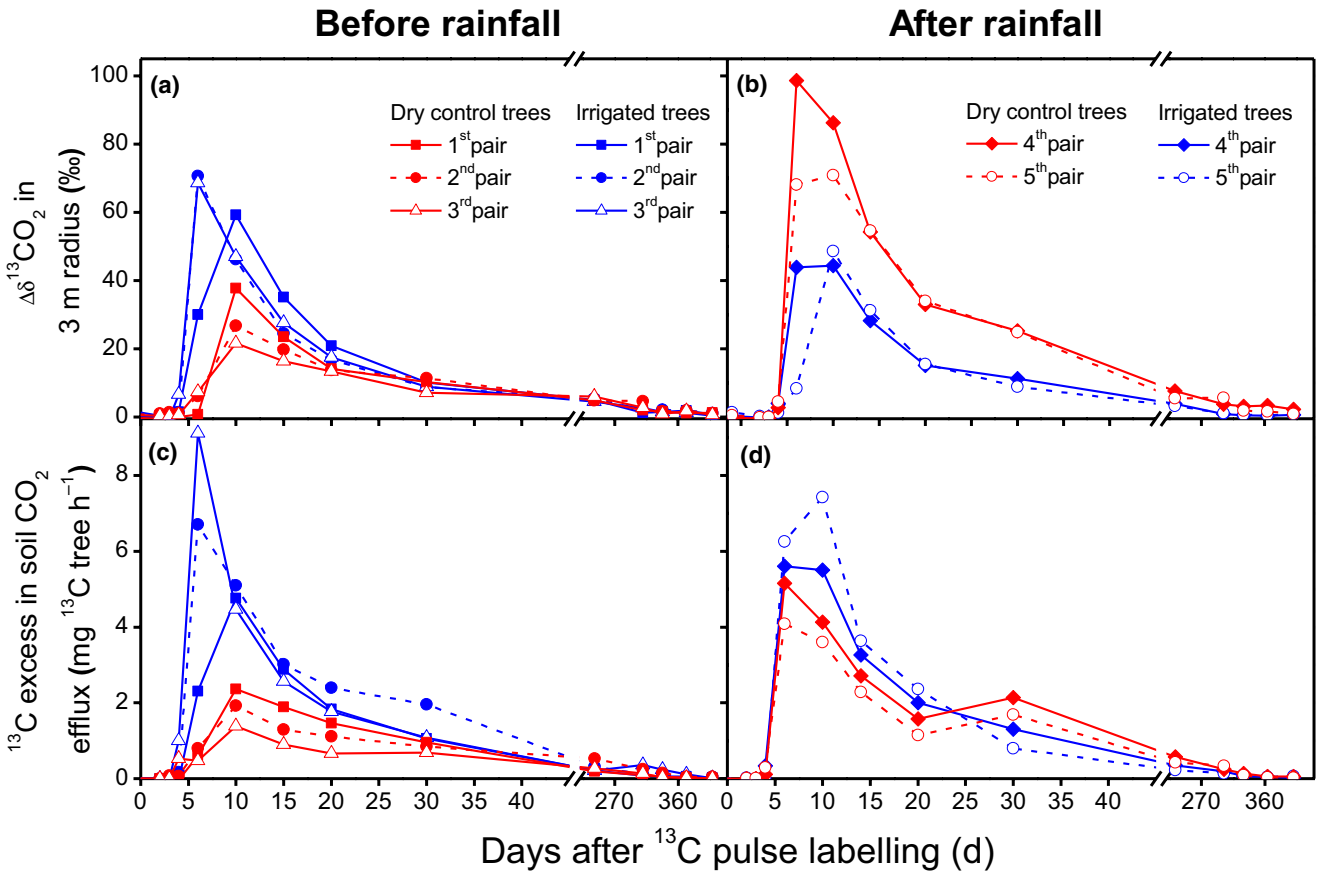

FIGURE 3 Temporal dynamics of the $\Delta\delta^{13}C$ values within 3-m distance from tree stems (upper two panels) and ^{13}C excess in soil CO_2 efflux of the entire area around the pulse-labelled trees (lower two panels) in the irrigated and the dry control treatments over more than a year. Three trees per treatment have been labelled in the time block before the rainfall event ((a) and (b)) and two trees per treatment have been labelled after the rainfall event at higher soil water contents ((c) and (d))

that of the tree crowns ($p < 0.01$), with the radii of the *maximal* and *active* rhizosphere extending on average 170% and 78% beyond the radii of the tree crowns respectively (Figure S3). Long-term irrigation affected the spatial distribution of the ^{13}C signal of soil-respired CO_2 (Table 2; Figures 7 and 8). On average, the *maximal* rhizosphere (confined by a detectable $\Delta\delta^{13}C\text{-}CO_2$ of 5‰) of irrigated trees reached 1.2 m further away from tree stems than the one of the dry control trees ($P_{Irrigation} < 0.05$). The radius of the *active* rhizosphere was 0.6 m larger in the irrigated trees. When scaled up to the area basis around tree stems, irrigation increased the *active* rhizosphere area by 60%. The ratio of rhizosphere to the crown area did, however, not change significantly with irrigation (Figure S3).

3.4 | ^{13}C excess in soil respiration

Relating $\Delta\delta^{13}C\text{-}CO_2$ to interpolated soil respiration rates and integrating ^{13}C signal in space and time yielded ^{13}C excess in soil-respired CO_2 for each of the pulse-labelled trees. For the first 10 days, irrigation increased the ^{13}C excess in soil-respired CO_2 ($P_{Irrigation} < 0.01$) but the effect size was greater for the pulse labelling carried out in the time block before than after the precipitation event (e.g. 370 vs. 35%; $P_{Timing \times Irrigation} < 0.05$). Relating the ^{13}C excess in soil-respired CO_2 to the amount of assimilated $^{13}CO_2$ for the first 10 days showed that long-term irrigation increased the allocation and use of recent assimilates not only in absolute but also in relative terms ($P_{Irrigation} < 0.05$). Overall, ^{13}C excess in soil-respired CO_2 showed a threshold type relationship with soil moisture (Figure 6). Moreover, it was positively related to the transport velocity of recent assimilates from the tree canopy to the rhizosphere (Figure 5). ^{13}C excess in root biomass showed a similar response pattern, but only *timing* was significant (Table 1).

On an annual timescale, irrigation increased ^{13}C excess in soil-respired CO_2 by 78% as compared to the dry control for the first pulse labelling before the precipitation event, due to the strong increase during the first 30 days. When pulse-labelled in the second time block after the precipitation event, at a higher soil moisture during pulse labelling, this effect disappeared ($P_{Timing \times Irrigation} = 0.051$). In relative terms, when compared with the ^{13}C uptake by trees, the ^{13}C losses by soil respiration averaged 30 ± 2% integrated over a year (Table 1; Figure S4). Respiratory ^{13}C losses were not significantly influenced by the water regime: the higher $^{13}CO_2$ flux from the soil in the irrigation treatment during the initial phase was compensated

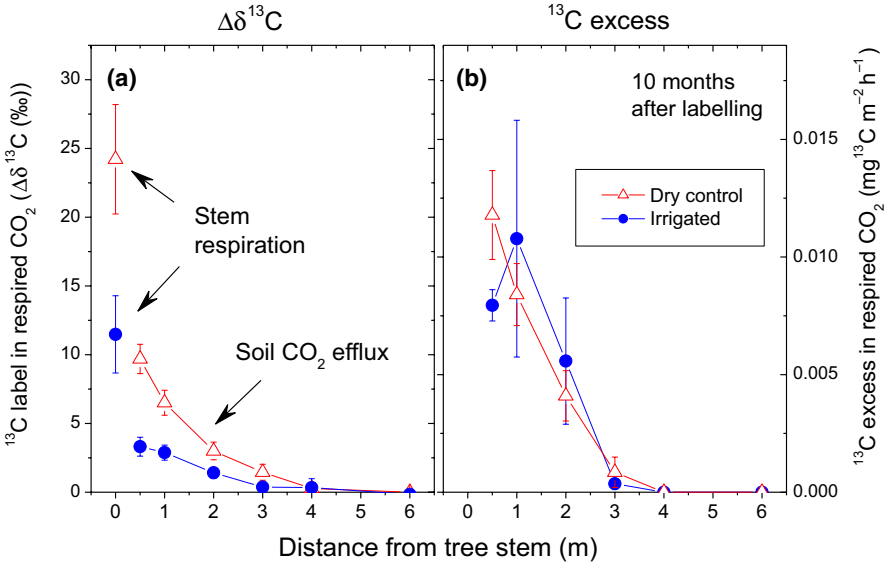

FIGURE 4 The $\Delta\delta^{13}C$ and ^{13}C excess in stem-respired CO_2 and soil-respired CO_2 10 months after pulse labelling in July 2018. Means and standard errors of five trees per treatment

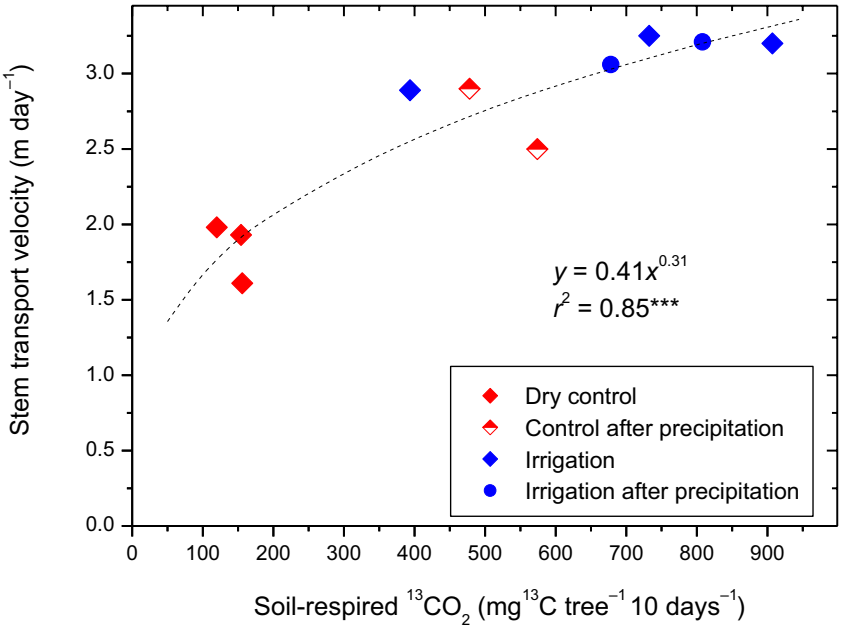

FIGURE 5 Relationship between soil-respired $^{13}CO_2$ and the transport velocity from the canopy to the rhizosphere in the pulse-labelled trees before and after the precipitation. The transport velocity depicts the time between $^{13}CO_2$ pulse labelling in the canopy of the approximately 12-m tall pine trees and its appearance in soil-respired CO_2

by a smaller $^{13}CO_2$ flux in later stages ($P_{Irrigation}$ = 0.002; Figure S4; Table 1).

3.5 | Spatio-temporal dynamics of ^{13}C in microbial biomass

The ^{13}C signal in soil microbial biomass C (MBC) also varied with time after labelling and soil depth (Figures 8 and 9). In the topsoil, the ^{13}C excess in MBC was highest down to 5 cm depth. In agreement with soil-respired CO_2, the ^{13}C excess in MBC started to appear 4 days and peaked approximately 10 days after pulse labelling (Figure 9). The irrigation effect on ^{13}C excess in MBC differed between the two time blocks of the pulse labelling ($P_{Timing \times Irrigation}$ = 0.002; Table 1). The ^{13}C excess in MBC averaged across all depth was 2.3 times greater under irrigation before the precipitation event, but 1.8 times smaller in irrigated soils after the precipitation event.

Total ^{13}C allocation from trees to the active rhizosphere, comprising respired CO_2 and microbial biomass, was 2.6 times greater in the irrigated than in the control trees before the precipitation event but only 1.3 times after it ($P_{Irrigation}$ = 0.004, Table 1). We also estimated the contribution of microbial biomass to the ^{13}C used in the rhizosphere (respired CO_2 and microbial C) until the ^{13}C peak, when further processing of microbial C can still be assumed to be small. Results showed that in relative terms microbial biomass incorporated greater fractions of recent assimilates in the dry control than in the irrigation

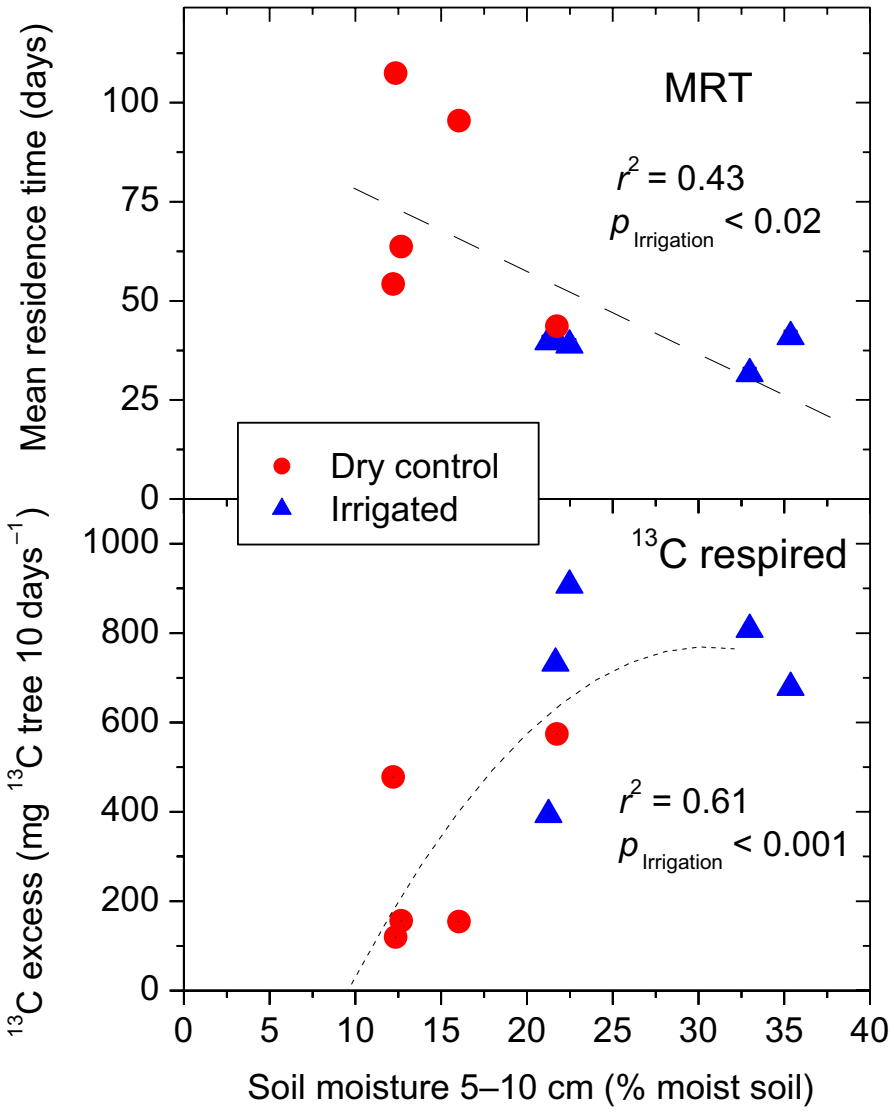

FIGURE 6 Relationships between soil moisture at 5–10 cm and mean residence time (MRT) from assimilation in tree canopies to soil respiration (top) as well as ^{13}C excess in soil-respired CO_2 in the irrigated and dry treatments over the first 10 days after pulse labelling. Each point represents the results from the integrated fluxes around one mature pine tree. Lines represent best fits to linear and polynomial functions

TABLE 2 Spatial patterns of soil-respired $^{13}CO_2$ following pulse labelling of mature trees, depicting the rhizosphere size. Active rhizosphere was defined to have a $^{13}CO_2$ signal strength of 25% of its maxima within the first m from each stem. Maximal lateral extension was confined to have a $\Delta\delta^{13}CO_2$ signal >5‰ that is significant. Values were reported as means ± standard errors

Timing	Treatment	Lateral extension (radius) active rhizosphere (m)	Maximal lateral extension (radius) rhizosphere (m)	Area of active rhizosphere (m^2)	Area of total rhizosphere (m^2)
Before precipitation	Irrigated	2.6 ± 0.12	3.8 ± 0.42	20.8 ± 2.0	46.1 ± 10.2
	Dry control	2.0 ± 0.19	2.9 ± 0.22	13 ± 1.1	26.1 ± 4.1
After precipitation	Irrigated	3.2 ± 0.55	5.3 ± 0.67	32.1 ± 0.5	55.6 ± 12.3
	Dry control	2.5 ± 0.155	3.6 ± 0.38	19.8 ± 0.1	41.7 ± 8.5
Statistical significance	Crown area	**0.0009**	0.17	**0.0009**	0.15
	Timing	0.09	0.088	0.09	0.87
	Irrigation	**0.01**	**0.042**	**0.01**	0.25
	Timing ×Irr.	0.15	0.59	0.15	0.544

Bold indicates significant values ($p < 0.05$).

treatment ($P_{Irrigation}$ = 0.019; Table 1). The fraction of ^{13}C processed in the rhizosphere that was incorporated into microbial biomass was 47% in the dry control and 31% in the irrigated treatment.

4 | DISCUSSION

Our ^{13}C pulse-labelling experiment with mature trees documents the 'carbon footprint' of trees in forest soils—recent photosynthates

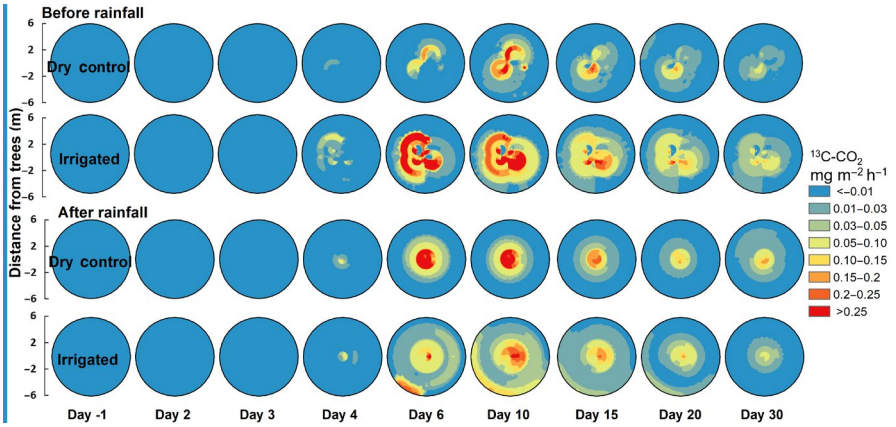

FIGURE 7 Spatio-temporal dynamics of ^{13}C excess in soil-respired CO_2 under the canopy of the mature pine trees in the dry control and irrigation treatment in the time block before (two upper rows) and after (two lower rows) the intermittent rainfall event. The tree stems are in the middle of each circle and tree canopies have an average radius of 1.29 ± 0.17 m and 1.52 ± 0.21 in the dry control and irrigated treatment respectively

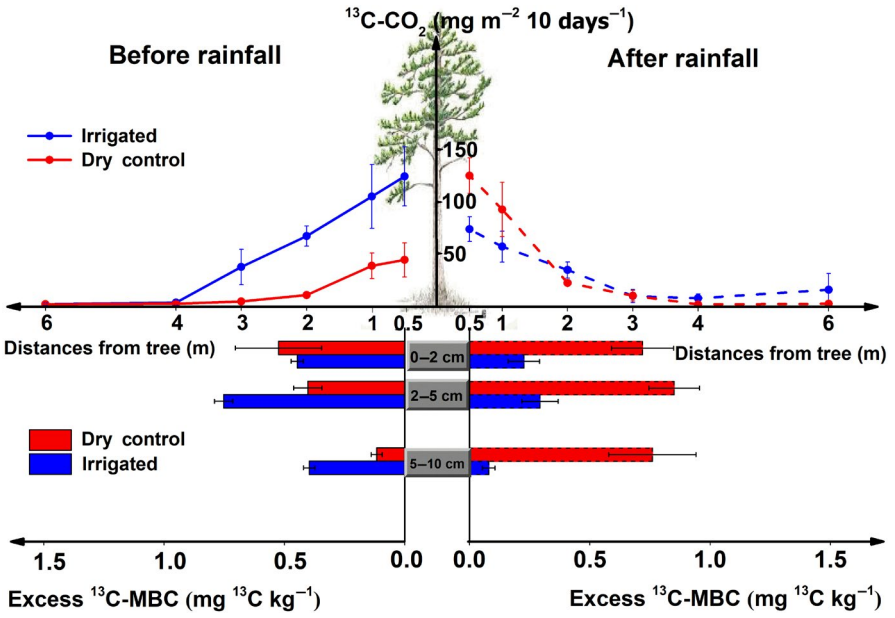

FIGURE 8 Cumulative flux of soil-respired $^{13}CO_2$ (^{13}C excess) during the first 10 days following pulse labelling, and ^{13}C excess in microbial biomass carbon (MBC) at 0–2, 2–5 and 5–10 cm depth 10 days after pulse labelling. Means and standard errors of three mature pine trees per treatment in the time block before the rainfall event and two trees per treatment in the time block after the rainfall event

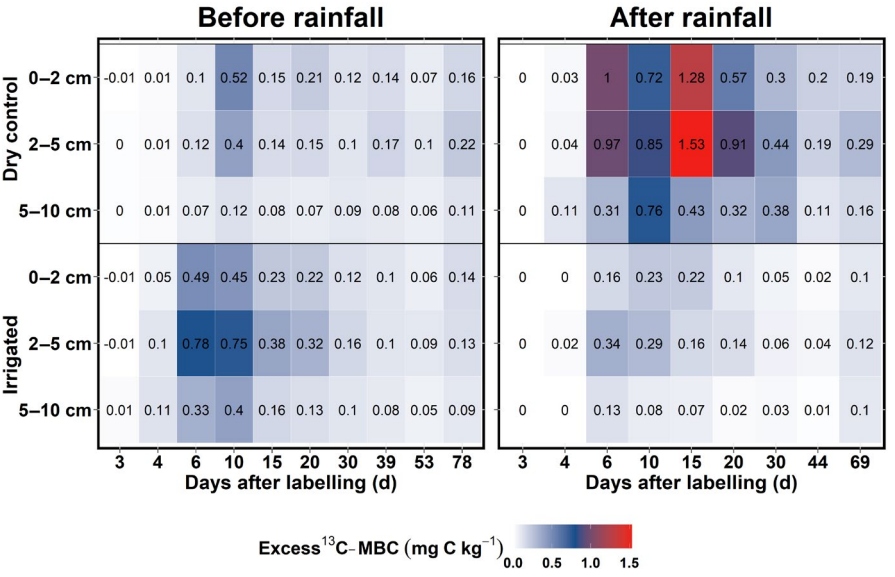

FIGURE 9 Spatio-temporal dynamics of ^{13}C excess in microbial biomass following pulse labelling of mature pine trees before and after a rainfall event. The heat map shows the ^{13}C excess at 0–2, 2–5 and 5–10 cm soil depth under the irrigated treatment and the naturally dry control within the first m distance from the trees

arrived 4 to 6 days after their assimilation in the rhizosphere, where they were rapidly transferred to soil microbial communities but still used for respiratory processes 1 year after their original assimilation. Most importantly, our results show that soil moisture status alters the spatio-temporal pattern of the C flow from the above into the belowground that will impact a multitude of ecosystem processes.

4.1 | Spatio-temporal dynamics of rhizosphere respiration

The time lag of a few days between $^{13}CO_2$ uptake and rhizosphere respiration give evidence of a rather intimate coupling of the above- and belowground C cycle in this mature forest. However, these time spans observed in the 12-m tall and approximately 100-year-old pine trees are substantially greater than in previous whole tree pulse-labelling experiments with similarly sized but younger trees (Epron et al., 2011), showing time lags of only 0.5 to 1.3 days for 15- and 20-year-old oak and beech trees and 1.6 to 2.7 days for 12-year-old maritime pine trees. The different velocities of C transfer between beech and oak, on the one hand, and pine, on the other hand, likely reflect differences in phloem anatomy (Dannoura et al., 2011; Epron et al., 2012). Vessel sizes promoting a more rapid transport are generally larger in broadleaf than in conifer trees. Moreover, phloem transport rates have been shown to be greater in faster than in slower growing trees (Deslauriers et al., 2017) potentially explaining the differences between the pine trees in the experiments of Dannoura et al. (2011) and our trees. In boreal Scots pine (c. 14-year-old and 4-m tall), ^{13}C tracer arrived 1 day after pulse labelling and peaked 1–3 days thereafter (Högberg et al., 2008). Our pulse-labelling experiment revealed that the velocity of assimilate transport from the canopy of the mature pine trees to their rhizosphere is closely linked to the respiratory use of these assimilates in the rhizosphere (Figure 5), suggesting that the balance between C supply by assimilation and C use in sink tissues not only determines where C is allocated (see e.g. Hagedorn et al., 2016) but also how fast. The belowground C demand arises from the metabolic activity of roots, associated mycorrhizal fungi and soil microorganisms feeding on root exudates (Epron et al., 2012; Högberg et al., 2010; Kuzyakov & Gavrichkova, 2010). In our study, the ^{13}C label arrived at a similar time in soil extractable organic C and microbial C than in soil-respired CO_2 (Figure 9), supporting previous findings that recent photosynthates allocated to the roots are rapidly transferred to the soil and their microbial communities (e.g. von Rein et al. 2016). After its peak 10 days after pulse labelling, the ^{13}C signal in microbial biomass declined strongly, implying that the new microbial C was processed further and replaced by more recent but unlabelled assimilates. The quantitative importance of root exudation and respiratory processes in roots, associated symbionts and microbial communities remains largely elusive until now (Wang et al., 2021). Here, we could show that at the ^{13}C peak 10 days after pulse labelling, microbial biomass constituted between 28% and 49% of assimilates processed in the rhizosphere, that is, soil-respired CO_2 and microbial biomass. The ^{13}C incorporation into microbial biomass is likely an underestimate as it comprises only the uppermost 10 cm of the soil, which, however, constituted 70% of the entire soil organic C stock and 60% of fine root biomass (Brunner et al. 2019; Hartmann et al., 2017). Nonetheless, our estimate is in agreement with the separation of various components of soil respiration in an oak forest, showing that approximately 30% of the annual autotrophic respiration originated from mycorrhizal respiration with a stronger contribution in late summer (Heinemeyer et al., 2011).

The long-term ^{13}C tracking—detecting the ^{13}C label of the 3.5-h pulse-labelling experiment 1 year later—gives evidence that soil CO_2 effluxes in forests reflect an integral of plant-derived C with residence times ranging from days to years. This supports the conceptual model of Kuzyakov and Gavrichkova (2010) that time lags between photosynthesis and soil respiration reflect the various sources of soil-respired CO_2. The continuous respiratory use of pre-aged C detected here can be attributed to two dominant pathways: (1) On the one hand, it can originate from a storage pool in trees, where assimilates are transiently stored before they are used for metabolic processes years later (Herrera-Ramírez et al., 2020). (2) Alternatively, the ^{13}C signal in soil-respired CO_2 could result from the turnover of fine roots and their associated microorganism that have incorporated the ^{13}C signal of the pulse labelling and slowly decompose in the following year. In our study, the strong ^{13}C signal in stem-respired CO_2 after 10 months (Figure 4) gives clear evidence that assimilates are still used for tree metabolism and hence it also seems likely that they are continuously allocated to the rhizosphere. This is supported by the ^{14}C-based findings that new fine roots consist of several years old C (Solly et al., 2018), showing that pre-aged C is in fact allocated and used in the rhizosphere.

The spatial mapping of the ^{13}C signal in soil-respired CO_2 documents that recent photosynthates were distributed and used for respiratory processes in a radius of 3 to 6 m around individual tree stems—a lateral extension that falls into the range of empirical estimates of the fine root distribution around trees (Schwarz et al., 2010). The values also agree with a 5-m wide radius of the fine root system measured for 12-m tall loblolly pine trees based on the distinct ^{13}C signature from long-term CO_2 enrichment (Johnsen et al., 2005). The hot spots at the outermost distance from the tree trunk observed in our study indicate that few roots or associated mycorrhizal fungi may also extend beyond this range, but given that such hot spots were found in only one of the 10 pulse-labelled trees, this appears to be rather the exception. Our finding that the spatial extension of the rhizosphere respiration corresponds approximately to twice the size of tree crown projection area implies that in this pine forest with a canopy cover of 70% in the dry control and 90% in the irrigated plots and an average distance between tree stems of 4.1 m, there is a strong overlap of the rhizosphere among adjacent trees and thus an intense exploitation of resources and competition in the soil (Brunner et al., 2004; Göttlicher et al., 2008).

4.2 | Soil moisture alters short and long-term rhizosphere dynamics

The drought regime—ranging from a moderate water shortage in the dry control, its short-term modulation by small precipitation events and its experimental removal by long-term irrigation—clearly affected the spatio-temporal pattern of rhizosphere respiration. Water limitation altered the allocation and use of recent assimilates in the

rhizosphere at various timescales, reaching from immediate effects on rhizosphere respiration to indirect effects through an enlarged rooting system developed over several years.

1. *At the daily to weekly timescale*, the amount of ^{13}C respired from the soils was significantly greater in the irrigation treatment, indicating that naturally dry conditions before the precipitation event restricted the allocation of recent assimilates to the belowground. This is consistent with drought experiments in grasslands and with young trees (Fuchslueger et al., 2014; Hagedorn et al., 2016), for which there are two potential mechanisms: water limitation either decreases CO_2 assimilation through photosynthesis and thus reduces the C availability inducing a 'source limitation', or suppresses the 'sink' activity in the rhizosphere where dry conditions reduce the metabolization of assimilates. This reduction in demand in turn feeds back on photosynthesis (Gessler & Grossiord, 2019; Hagedorn et al., 2016). In our experiment conducted under a natural moderate drought, the whole crown assimilation of the ^{13}C tracer as well as leaf-level photosynthesis remained unaffected by irrigation (Joseph et al., 2020), which indicates that a limited sink activity in the rhizosphere was primarily responsible for the reduced rhizosphere respiration in dry soils. This conclusion is corroborated by the relatively greater incorporation of recent assimilates into microbial biomass (as compared to respiratory activity in the rhizosphere) in dry compared to irrigated soils (46 vs. 31%), signifying that the metabolization of assimilates is most strongly constrained by water.

   Our results show that intermittent precipitation events can strongly alter the dynamics and allocation patterns of recent assimilates from tree canopies into the soil. While drought retarded and suppressed the ^{13}C signal in soil respiration before the intermittent precipitation event, assimilates were transported faster afterwards. In the dry control treatment, increased soil moisture as a consequence of light rainfall increased the ^{13}C signal in root biomass, soil-respired CO_2, in EOC and in soil microbial biomass as compared to the previous drier conditions and even surpassed the permanent moist irrigation treatment in the case of microbial biomass. We attribute this switch primarily to a removal of water limitation for metabolic activity in the surface soils of the dry control by the precipitation event. Here, soil moisture contents ranged around 15% (volumetric and gravimetric water contents per moist soil) which is congruent with reported critical thresholds values for microbial activity (e.g. Manzoni et al., 2012). Hence, the slight increase in soil moisture by the intermittent rainfall pushed this biologically most active soil layer with the highest densities of fine roots (Brunner et al., 2019) and microbial biomass above this threshold and led to an increased respiratory activity of the rhizosphere and their associated microorganisms (Joseph et al., 2020). The moisture-induced increase in the belowground sink activity seemed also to be linked to the transport velocity of assimilates in tree stems, suggesting that an enhanced use of assimilates by the rhizobiome following rewetting may rapidly feeds back on the allocation of photosynthates within mature trees.

   As the precipitation event occurred shortly after the first time block of pulse labelling, it might have also affected the allocation patterns of C assimilated by trees in this block. However, the ^{13}C signal in soil-respired CO_2 and microbial biomass remained small, which suggests that the initial allocation (that occurred before the rain event and its effect on soil water contents) seems decisive for the distribution of assimilates in trees and how much of them are transferred to the soil. Overall, the ^{13}C tracing indicates that C allocation within entire 100-year-old trees coupling the above- and belowground system is highly sensitive to small changes in soil moisture around critical threshold values for the rhizobiome activity. Under sufficient moisture, the enhanced use of assimilates by the rhizobiome induces an increased allocation of recent assimilates to the rhizobiome. Vice versa, drying of surface soils below critical moisture levels for microorganisms will decrease the sink activity of the rhizobiome already at moderate drought levels that are not critical for tree vitality, as trees are able to access water also from deeper soil layers, which has consequences for allocation and probably also the processing of assimilates within trees.
2. *Annual timescale*. In the year following the ^{13}C pulse labelling, irrigation decreased the $\Delta\delta^{13}C\text{-}CO_2$ signal of transiently stored assimilates in soil-respired CO_2, but as soil respiration rates were increased to a similar extent, the respiratory losses of pre-aged assimilates remained unaffected by irrigation in quantitative terms. This pattern indicates that the isotopic signal of the 1-year-old C was diluted by a greater respiratory activity in moist soils—either by a stronger allocation and respiratory use of 'younger' but now unlabelled assimilates in the soil as observed during the initial phase of the pulse labelling the year before or by an enhanced release of 'older', more than 1-year-old C through an accelerated mineralization of soil organic matter.
3. *Decadal timescale*. While the ^{13}C signal intensity reflects the daily to annual moisture effects on the C allocation from tree canopies into the soil, the spatial pattern mirrors the long-term acclimation of trees to soil moisture regimes. Our spatial mapping of the ^{13}C signal showed that irrigation enlarged the lateral extent of the rhizosphere respiration by approximately 30%, which when scaled up to an area basis indicates that the removal of summer moisture limitation for more than decade increased the overall 'footprint' area of each tree by 60%. The substantially greater rhizosphere of irrigated trees is consistent with the fine root biomass that has continuously increased over the years reaching an 80% greater biomass after 13 years (1 year before this pulse-labelling experiment; Brunner et al., 2019). In addition, the extension may result from an enlarged mycorrhizal network as observed in other drought experiments (Hagedorn et al., 2016). The increased fine root biomass and rhizosphere expansion of irrigated trees are in agreement with other water manipulation experiments showing smaller fine root biomass under drought conditions, very likely in

response to the reduced aboveground C assimilation and the high C costs for forming roots (Brunner et al., 2015). In this pine forest, the aboveground growth of pine trees was also clearly enhanced by the experimental removal of water limitation (Hartmann et al., 2017; Rigling et al., 2013). In conjunction with our observation that rhizosphere area parallels canopy size, this strongly suggests that trees adjust their rhizosphere system to the resources available (carbon, water and nutrients). Somewhat counter-intuitively, under ambient dry conditions repeatedly leading to tree mortality, trees appear not capable to invest in their rhizosphere at least not in absolute terms although it would be beneficial to their water and nutrient supply. This pattern might be different under mild drought or in response to a single drought event where drought is observed to enhance fine root production (Gaul et al., 2008), especially upon recovery from drought (Hagedorn et al., 2016).

The moisture-dependent belowground C allocation at the daily to decadal timescale has consequences for soil microbial communities and soil carbon cycling (Canarini et al., 2017). In our long-term experiment, irrigation increased the labile soil organic matter pool and shifted the microbiome from a largely oligotrophic to a more copiotrophic life strategy (Hartmann et al., 2017). However, it remains uncertain to which extent the enhanced C inputs into soil organic matter are balanced out by an accelerated microbial decomposition under continuously moist conditions.

5 | CONCLUSION

Our whole tree pulse-labelling experiment in a mature forest documents that the drought regime affects the coupling of the above- and belowground system and the feedback between plant and soil processes at various timescales. The spatio-temporal ^{13}C tracing in the soil gives evidence for an allocation of recent assimilates from tree canopies to the rhizosphere and associated microbial communities within days, but also for a retarded C transfer for more than a year through intermediate C storage within trees. Rhizosphere respiration responded highly sensitive to the 15-year long-term irrigation and the intermittent rainfall event. We suggest that the modulation of rhizosphere respiration by soil moisture plays a decisive role in C allocation in trees under moderate drought. The reduced C sink activity of roots and associated mycorrhizae and microbial communities below critical moisture contents appear to reduce the velocity and the amount of assimilates allocated to the belowground. This effect is amplified by the long-term acclimation of trees to repeated summer droughts, with a reduced growth and thus spatial extension of the rhizosphere system. Potentially, the reduced sink strength in the belowground in dry soils feeds back on tree's CO_2 uptake and the allocation and processing of assimilates in trees. In the rhizosphere, the decreased C supply from trees under drought has consequences not only for the microbial activity in the short term, but also for soil microbial community and soil C storage in the longer term. Predictions on the interplay of these interlinked above and belowground processes are hampered by non-linear responses of these processes to soil moisture, frequently unknown depth patterns of fine roots and their associated rhizobiome and the great temporal variability of soil moisture in the three-dimensional soil space.

ACKNOWLEDGEMENTS

This study was based on the long-term irrigation experiment Pfynwald, which is part of the Swiss Long-term Forest Ecosystem Research Programme LWF (www.lwf.ch). It was funded by the Sino Swiss Science and Technology Cooperation (EG09-122016) (to D. G. and F. H.) and the Swiss National Science Foundation (SNF) under contract numbers 31003A_159866 and 310030_189109 (to A.G.). The authors are grateful to A. Rigling for initiating the long-term irrigation experiment, M. Schaub and P. Bleuler for maintaining it, M. Saurer, C. Poll, H. Hartmann, G. Gleixner, Mai-He Li, B. Backes, F.M. Thomas, W. Werner, J. Luster and M.M. Lehmann for contributing to the pulse-labelling experiment, and U. Graf and A. Schlumpf for analysing stable isotopes. They also thank three anonymous reviewer for their constructive comments.

CONFLICT OF INTEREST

None is declared.

AUTHOR CONTRIBUTIONS

F.H., D.G., A.G., J.J. and E.B. designed the study; D.G., F.H., J.J., R.A.W., I.B., A.Z., C.H., A.W. and K.M. performed the pulse-labelling experiment and analysed the samples; D.G., F.H. and C.Z. performed the data analysis; F.H., D.G. and A.G. wrote the manuscript with all authors contributing.

DATA AVAILABILITY STATEMENT

The data that support the findings of this study are openly available in www.envidat.ch at https://doi.org/10.16904/envidat.209.

ORCID

Decai Gao https://orcid.org/0000-0003-0545-4020
Jobin Joseph https://orcid.org/0000-0002-6342-2505
Roland A Werner https://orcid.org/0000-0002-4117-1346
Ivano Brunner https://orcid.org/0000-0003-3436-995X
Ao Wang https://orcid.org/0000-0002-0140-8468
Chunhong Zhao https://orcid.org/0000-0003-0391-6420
Edith Bai https://orcid.org/0000-0003-0495-6504
Katrin Meusburger https://orcid.org/0000-0003-4623-6249
Arthur Gessler https://orcid.org/0000-0002-1910-9589
Frank Hagedorn https://orcid.org/0000-0001-5218-7776

REFERENCES

Barthel, M., Hammerle, A., Sturm, P., Baur, T., Gentsch, L., & Knohl, A. (2011). The diel imprint of leaf metabolism on the $\delta^{13}C$ signal of soil respiration under control and drought conditions. *New Phytologist*, *192*(4), 925–938. https://doi.org/10.1111/j.1469-8137.2011.03848.x

Bigler, C., Bräker, O. U., Bugmann, H., Dobbertin, M., & Rigling, A. (2006). Drought as an inciting mortality factor in Scots Pine stands of

the Valais, Switzerland. *Ecosystems*, *9*(3), 330–343. https://doi.org/10.1007/s10021-005-0126-2

Brunner, I., Herzog, C., Dawes, M. A., Arend, M., & Sperisen, C. (2015). How tree roots respond to drought. *Frontiers in Plant Science*, *6*, 547. https://doi.org/10.3389/fpls.2015.00547

Brunner, I., Herzog, C., Galiano, L., & Gessler, A. (2019). Plasticity of fine-root traits under long-term irrigation of a water-limited Scots Pine forest. *Frontiers in Plant Science*, *10*, 701. https://doi.org/10.3389/fpls.2019.00701

Brunner, I., Ruf, M., Lüscher, P., & Sperisen, C. (2004). Molecular markers reveal extensive intraspecific below-ground overlap of silver fir fine roots. *Molecular Ecology*, *13*(11), 3595–3600. https://doi.org/10.1111/j.1365-294X.2004.02328.x

Buras, A., Rammig, A., & Zang, C. S. (2020). Quantifying impacts of the drought 2018 on European ecosystems in comparison to 2003. *Biogeosciences*, *17*(6), 1655–1672. https://doi.org/10.5194/bg-17-1655-2020

Canarini, A., Kiær, L. P., & Dijkstra, F. A. (2017). Soil carbon loss regulated by drought intensity and available substrate: A meta-analysis. *Soil Biology and Biochemistry*, *112*, 90–99. https://doi.org/10.1016/j.soilbio.2017.04.020

Ciais, P. H., Reichstein, M., Viovy, N., Granier, A., Ogée, J., Allard, V., Aubinet, M., Buchmann, N., Bernhofer, C., Carrara, A., Chevallier, F., De Noblet, N., Friend, A. D., Friedlingstein, P., Grünwald, T., Heinesch, B., Keronen, P., Knohl, A., Krinner, G., … Valentini, R. (2005). Europe-wide reduction in primary productivity caused by the heat and drought in 2003. *Nature*, *437*(7058), 529–533. https://doi.org/10.1038/nature03972

Dannoura, M., Maillard, P., Fresneau, C., Plain, C., Berveiller, D., Gerant, D., Chipeaux, C., Bosc, A., Ngao, J., Damesin, C., Loustau, D., & Epron, D. (2011). *In situ* assessment of the velocity of carbon transfer by tracing ^{13}C in trunk CO_2 efflux after pulse labelling: Variations among tree species and seasons. *New Phytologist*, *190*(1), 181–192. https://doi.org/10.1111/j.1469-8137.2010.03599.x

Deslauriers, A., Fonti, P., Rossi, S., Rathgeber, C. B. K., & Gričar, J. (2017). Ecophysiology and plasticity of wood and phloem formation. In M. Amoroso, L. Daniels, P. Baker & J. Camarero (Eds.), *Dendroecology*. Ecological studies (analysis and synthesis) (Vol. *231*). Springer. https://doi.org/10.1007/978-3-319-61669-8_2

Epron, D., Bahn, M., Derrien, D., Lattanzi, F. A., Pumpanen, J., Gessler, A., Hogberg, P., Maillard, P., Dannoura, M., Gerant, D., & Buchmann, N. (2012). Pulse-labelling trees to study carbon allocation dynamics: A review of methods, current knowledge and future prospects. *Tree Physiology*, *32*(6), 776–798. https://doi.org/10.1093/treephys/tps057

Epron, D., Ngao, J., Dannoura, M., Bakker, M. R., Zeller, B., Bazot, S., & Loustau, D. (2011). Seasonal variations of belowground carbon transfer assessed by in situ $^{13}CO_2$ pulse labelling of trees. *Biogeosciences*, *8*(5), 1153–1168. https://doi.org/10.5194/bg-8-1153-2011

Frank, D., Reichstein, M., Bahn, M., Thonicke, K., Frank, D., Mahecha, M. D., Smith, P., Velde, M., Vicca, S., Babst, F., Beer, C., Buchmann, N., Canadell, J. G., Ciais, P., Cramer, W., Ibrom, A., Miglietta, F., Poulter, B., Rammig, A., … Zscheischler, J. (2015). Effects of climate extremes on the terrestrial carbon cycle: Concepts, processes and potential future impacts. *Global Change Biology*, *21*(8), 2861–2880. https://doi.org/10.1111/gcb.12916

Fuchslueger, L., Bahn, M., Fritz, K., Hasibeder, R., & Richter, A. (2014). Experimental drought reduces the transfer of recently fixed plant carbon to soil microbes and alters the bacterial community composition in a mountain meadow. *New Phytologist*, *201*(3), 916–927. https://doi.org/10.1111/nph.12569

Fuchslueger, L., Bahn, M., Hasibeder, R., Kienzl, S., Fritz, K., Schmitt, M., Watzka, M., & Richter, A. (2016). Drought history affects grassland plant and microbial carbon turnover during and after a subsequent drought event. *Journal of Ecology*, *104*(5), 1453–1465. https://doi.org/10.1111/1365-2745.12593

Gaul, D., Hertel, D., Borken, W., Matzner, E., & Leuschner, C. (2008). Effects of experimental drought on the fine root system of mature Norway spruce. *Forest Ecology and Management*, *256*(5), 1151–1159. https://doi.org/10.1016/j.foreco.2008.06.016

Gessler, A., & Grossiord, C. (2019). Coordinating supply and demand: Plant carbon allocation strategy ensuring survival in the long run. *New Phytologist*, *222*(1), 5–7. https://doi.org/10.1111/nph.15583

Gessler, A., Schaub, M., & McDowell, N. G. (2017). The role of nutrients in drought-induced tree mortality and recovery. *New Phytologist*, *214*(2), 513–520. https://doi.org/10.1111/nph.14340

Göttlicher, S. G., Taylor, A. F. S., Grip, H., Betson, N. R., Valinger, E., Högberg, M. N., & Högberg, P. (2008). The lateral spread of tree root systems in boreal forests: Estimates based on ^{15}N uptake and distribution of sporocarps of ectomycorrhizal fungi. *Forest Ecology and Management*, *255*(1), 75–81. https://doi.org/10.1016/j.foreco.2007.08.032

Hagedorn, F., Joseph, J., Peter, M., Luster, J., Pritsch, K., Geppert, U., Kerner, R., Molinier, V., Egli, S., Schaub, M., Liu, J.-F., Li, M., Sever, K., Weiler, M., Siegwolf, R. T. W., Gessler, A., & Arend, M. (2016). Recovery of trees from drought depends on belowground sink control. *Nature Plants*, *2*, 16111. https://doi.org/10.1038/nplants.2016.111

Hagedorn, F., Kammer, A., Schmidt, M. W. I., & Goodale, C. L. (2012). Nitrogen addition alters mineralization dynamics of ^{13}C-depleted leaf and twig litter and reduces leaching of older DOC from mineral soil. *Global Change Biology*, *18*(4), 1412–1427. https://doi.org/10.1111/j.1365-2486.2011.02603.x

Hartmann, M., Brunner, I., Hagedorn, F., Bardgett, R. D., Stierli, B., Herzog, C., Chen, X., Zingg, A., Graf-Pannatier, E., Rigling, A., & Frey, B. (2017). A decade of irrigation transforms the soil microbiome of a semi-arid pine forest. *Molecular Ecology*, *26*(4), 1190–1206. https://doi.org/10.1111/mec.13995

Heinemeyer, A., Di Bene, C., Lloyd, A. R., Tortorella, D., Baxter, R., Huntley, B., Gelsomino, A., & Ineson, P. (2011). Soil respiration: Implications of the plant-soil continuum and respiration chamber collar-insertion depth on measurement and modelling of soil CO_2 efflux rates in three ecosystems. *European Journal of Soil Science*, *62*(1), 82–94. https://doi.org/10.1111/j.1365-2389.2010.01331.x

Herrera-Ramírez, D., Muhr, J., Hartmann, H., Römermann, C., Trumbore, S., & Sierra, C. A. (2020). Probability distributions of nonstructural carbon ages and transit times provide insights into carbon allocation dynamics of mature trees. *New Phytologist*, *226*(5), 1299–1311. https://doi.org/10.1111/nph.16461

Herzog, C., Steffen, J., Graf Pannatier, E., Hajdas, I., & Brunner, I. (2014). Nine years of irrigation cause vegetation and fine root shifts in a water-limited pine forest. *PLoS One*, *9*(5), e96321. https://doi.org/10.1371/journal.pone.0096321

Högberg, M. N., Briones, M. J. I., Keel, S. G., Metcalfe, D. B., Campbell, C., Midwood, A. J., Thornton, B., Hurry, V., Linder, S., Näsholm, T., & Högberg, P. (2010). Quantification of effects of season and nitrogen supply on tree below-ground carbon transfer to ectomycorrhizal fungi and other soil organisms in a boreal pine forest. *New Phytologist*, *187*(2), 485–493. https://doi.org/10.1111/j.1469-8137.2010.03274.x

Högberg, P., Högberg, M. N., Göttlicher, S. G., Betson, N. R., Keel, S. G., Metcalfe, D. B., Campbell, C., Schindlbacher, A., Hurry, V., Lundmark, T., Linder, S., & Näsholm, T. (2008). High temporal resolution tracing of photosynthate carbon from the tree canopy to forest soil microorganisms. *New Phytologist*, *177*(1), 220–228. https://doi.org/10.1111/j.1469-8137.2007.02238.x

Hommel, R., Siegwolf, R., Zavadlav, S., Arend, M., Schaub, M., Galiano, L., Haeni, M., Kayler, Z. E., & Gessler, A. (2016). Impact of interspecific competition and drought on the allocation of new assimilates in trees. *Plant Biology*, *18*(5), 785–796. https://doi.org/10.1111/plb.12461

Johnsen, K., Maier, C., & Kress, L. (2005). Quantifying root lateral distribution and turnover using pine trees with a distinct stable carbon

isotope signature. *Functional Ecology*, *19*(1), 81–87. https://doi.org/10.1111/j.0269-8463.2005.00928.x

Joseph, J., Gao, D., Backes, B., Bloch, C., Brunner, I., Gleixner, G., Haeni, M., Hartmann, H., Hoch, G., Hug, C., Kahmen, A., Lehmann, M. M., Li, M.-H., Luster, J., Peter, M., Poll, C., Rigling, A., Rissanen, K. A., Ruehr, N. K., … Gessler, A. (2020). Rhizosphere activity in an old-growth forest reacts rapidly to changes in soil moisture and shapes whole-tree carbon allocation. *Proceedings of the National Academy of Sciences of the United States of America*, *117*(40), 24885–24892. https://doi.org/10.1073/pnas.2014084117

Kuzyakov, Y., & Gavrichkova, O. (2010). Review: Time lag between photosynthesis and carbon dioxide efflux from soil: A review of mechanisms and controls. *Global Change Biology*, *16*(12), 3386–3406. https://doi.org/10.1111/j.1365-2486.2010.02179.x

Lang, S. Q., Bernasconi, S. M., & Früh-Green, G. L. (2012). Stable isotope analysis of organic carbon in small (μg C) samples and dissolved organic matter using a GasBench preparation device. *Rapid Communications in Mass Spectrometry*, *26*(1), 9–16. https://doi.org/10.1002/rcm.5287

Manzoni, S., Schimel, J. P., & Porporato, A. (2012). Responses of soil microbial communities to water stress: Results from a meta-analysis. *Ecology*, *93*(4), 930–938. https://doi.org/10.1890/11-0026.1

Muhr, J., Angert, A., Negrón-Juárez, R. I., Muñoz, W. A., Kraemer, G., Chambers, J. Q., & Trumbore, S. E. (2013). Carbon dioxide emitted from live stems of tropical trees is several years old. *Tree Physiology*, *33*(7), 743–752. https://doi.org/10.1093/treephys/tpt049

Poorter, H., Niklas, K. J., Reich, P. B., Oleksyn, J., Poot, P., & Mommer, L. (2012). Biomass allocation to leaves, stems and roots: Meta-analyses of interspecific variation and environmental control. *New Phytologist*, *193*(1), 30–50. https://doi.org/10.1111/j.1469-8137.2011.03952.x

Reichstein, M., Bahn, M., Ciais, P., Frank, D., Mahecha, M. D., Seneviratne, S. I., Zscheischler, J., Beer, C., Buchmann, N., Frank, D. C., Papale, D., Rammig, A., Smith, P., Thonicke, K., van der Velde, M., Vicca, S., Walz, A., & Wattenbach, M. (2013). Climate extremes and the carbon cycle. *Nature*, *500*(7462), 287–295. https://doi.org/10.1038/nature12350

Rigling, A., Bigler, C., Eilmann, B., Feldmeyer-Christe, E., Gimmi, U., Ginzler, C., Graf, U., Mayer, P., Vacchiano, G., Weber, P., Wohlgemuth, T., Zweifel, R., & Dobbertin, M. (2013). Driving factors of a vegetation shift from Scots pine to pubescent oak in dry Alpine forests. *Global Change Biology*, *19*(1), 229–240. https://doi.org/10.1111/gcb.12038

Ruehr, N. K., Grote, R., Mayr, S., & Arneth, A. (2019). Beyond the extreme: Recovery of carbon and water relations in woody plants following heat and drought stress. *Tree Physiologist*, *39*(8), 1285–1299. https://doi.org/10.1093/treephys/tpz032

Ruehr, N. K., Offermann, C. A., Gessler, A., Winkler, J. B., Ferrio, J. P., Buchmann, N., & Barnard, R. L. (2009). Drought effects on allocation of recent carbon: From beech leaves to soil CO_2 efflux. *New Phytologist*, *184*(4), 950–961. https://doi.org/10.1111/j.1469-8137.2009.03044.x

Schimel, J. P. (2018). Life in dry soils: Effects of drought on soil microbial communities and processes. *Annual Review of Ecology, Evolution, and Systematics*, *49*(1), 409–432. https://doi.org/10.1146/annurev-ecolsys-110617-062614

Schönbeck, L., Gessler, A., Hoch, G., McDowell, N. G., Rigling, A., Schaub, M., & Li, M. H. (2018). Homeostatic levels of nonstructural carbohydrates after 13 yr of drought and irrigation in *Pinus sylvestris*. *New Phytologist*, *219*(4), 1314–1324. https://doi.org/10.1111/nph.15224

Schwarz, M., Lehmann, P., & Or, D. (2010). Quantifying lateral root reinforcement in steep slopes – From a bundle of roots to tree stands. *Earth Surface Processes and Landforms*, *35*(3), 354–367. https://doi.org/10.1002/esp.1927

Solly, E. F., Brunner, I., Helmisaari, H.-S., Herzog, C., Leppälammi-Kujansuu, J., Schöning, I., Schrumpf, M., Schweingruber, F. H., Trumbore, S. E., & Hagedorn, F. (2018). Unravelling the age of fine roots of temperate and boreal forests. *Nature Communications*, *9*(1), 3006. https://doi.org/10.1038/s41467-018-05460-6

Stocker, T. F., Qin, D., Plattner, G. K., Tignor, M. M., Allen, S. K., Boschung, J., Nauels, A., Xia, Y., Bex, V., & Midgley, P. M. (2014). Climate change 2013: The physical science basis. In *Contribution of working group I to the fifth assessment report of IPCC the intergovernmental panel on climate change*. Cambridge University Press. https://doi.org/10.1017/CBO9781107415324

Vance, E. D., Brookes, P. C., & Jenkinson, D. S. (1987). An extraction method for measuring soil microbial biomass C. *Soil Biology and Biochemistry*, *19*(6), 703–707. https://doi.org/10.1016/0038-0717(87)90052-6

von Rein, I., Gessler, A., Premke, K., Keitel, C., Ulrich, A., & Kayler, Z. E. (2016). Forest understory plant and soil microbial response to an experimentally induced drought and heat-pulse event: The importance of maintaining the continuum. *Global Change Biology*, *22*(8), 2861–2874. https://doi.org/10.1111/gcb.13270

Wang, R., Bicharanloo, B., Shirvan, M. B., Cavagnaro, T. R., Jiang, Y., Keitel, C., & Dijkstra, F. A. (2021). A novel ^{13}C pulse-labelling method to quantify the contribution of rhizodeposits to soil respiration in a grassland exposed to drought and nitrogen addition. *New Phytologist*. https://doi.org/10.1111/nph.17118

Zeeman, M. J., Werner, R. A., Eugster, W., Siegwolf, R. T., Wehrle, G., Mohn, J., & Buchmann, N. (2008). Optimization of automated gas sample collection and isotope ratio mass spectrometric analysis of $\delta^{13}C$ of CO_2 in air. *Rapid Communications in Mass Spectrometry*, *22*(23), 3883–3892. https://doi.org/10.1002/rcm.3772

SUPPORTING INFORMATION

Additional supporting information may be found online in the Supporting Information section.

How to cite this article: Gao D, Joseph J, Werner RA, et al. Drought alters the carbon footprint of trees in soils—tracking the spatio-temporal fate of ^{13}C-labelled assimilates in the soil of an old-growth pine forest. *Glob Change Biol*. 2021;27:2491–2506. https://doi.org/10.1111/gcb.15557